Published in final edited form as:

Immunol Cell Biol. 2010 ; 88(3): 334–342. doi:10.1038/icb.2009.107.

VCAM-1 blockade delays disease onset, reduces disease severity and inflammatory cells in an atopic dermatitis model

Lin Chen[*], **Shao-xia Lin**[*], **Sanober Amin**[*], **Lut Overbergh**[¶], **Giacomo Maggiolino**[*], and **Lawrence S. Chan**[*,†,‡]

[*]Dept of Dermatol, Univ. of Illinois, Chicago, IL, USA

[†]Dept of Micro/Immunol, Univ. of Illinois, Chicago, IL, USA

[¶]Lab Exp Med and Endocrinol, Catholic University of Leuven, Leuven, Belgium

[‡]Medicine Service, VA Jesse Brown Medical Center, Chicago, IL, USA

Abstract

We investigated the roles of critical adhesion molecules ICAM-1 and VCAM-1 in a keratin-14 IL-4 transgenic (Tg) mouse model of atopic dermatitis, the skin lesions of which are characterized by prominent inflammatory cell infiltration, significantly increased mRNAs and proteins of ICAM-1, VCAM-1, E-selectin, P-selectin, L-selectin, and PSGL-1, and significantly increased numbers of dermal vessels expressing these adhesion molecules. We tested the hypotheses that deletion or blockade of these molecules may impede the inflammation by examining the disease progresses in the Tg mice crossed with ICAM-1 knockout mice and Tg mice received anti-VCAM-1 neutralizing antibody. While the findings of the ICAM-1-knockout Tg mice (Tg/ICAM-1−/−) developed skin lesions similar to wide type ICAM-1 Tg mice (Tg/ICAM-1+/+) were surprising, a compensatory mechanism may account for it: the frequency of VCAM-1 ligand, CD49d, on CD3+ T cells in the lesional skin significantly increased in the Tg/ICAM-1−/− mouse, compared to the Tg/ICAM-1+/+ mice. By contrast anti-VCAM-1-treated Tg/ICAM-1−/− or Tg/ICAM-1+/+ mice had significantly delayed onset of skin inflammation compared to isotype antibody-treated groups. Moreover, anti-VCAM-1 significantly reduced the skin inflammation severity in Tg/ICAM-1+/+ mice, accompanied with reduction of mast cell, eosinophil, and CD3+ T-cell infiltration. VCAM-1 is more critical in developing skin inflammation in this model.

Keywords

atopic dermatitis; inflammation; ICAM-1; VCAM-1

Address correspondence to: Lawrence S. Chan, M.D., UIC-Dermatology, MC624, 808 S. Wood Street, Room 380, Chicago, IL 60612; Tel. (312) 996-6966; Fax. (312) 996-1188; larrycha@uic.edu.

Conflict of interest

The authors state no conflict of interest.

Introduction

Atopic dermatitis (AD) is a common, chronically relapsing, debilitating, pruritic, inflammatory skin disorder. AD usually starts during early infancy and childhood, but it can persist into or onset in adulthood. The prevalence of AD is 10–20% in children and 1–3% in adults and has increased 2- to 3 fold in the past three decades in developed countries 1. The major infiltrate of inflammatory cells in the skin lesions of AD are T cells, accompanied by macrophages, mast cells, and eosinophils 2–4. It is now well recognized that the cutaneous recruitment of leukocytes is a sophisticated process which involves a few groups of adhesion molecules including the selectins (E-selectin/P-selectin expressed on endothelial cells and L-selectin presented on almost all circulating leukocytes), immunoglobulin superfamily (ICAM and VACM expressed primarily on endothelial cells), and the integrins [$\alpha_4\beta_1$-integrin (very late antigen-4, VLA-4), $\alpha_5\beta_1$-integrin (very late antigen-5, VLA-5), $\alpha_L\beta_2$-integrin (lymphocyte function-associated antigen-1, LFA-1), and $\alpha_M\beta_2$ -integrin (Mac-1)] expressed on leukocytes 5. The leukocyte adhesion and extravasation cascade is a multistep process. In the first step that involves leukocyte tethering and rolling on the vessel wall, the transient adhesion interaction is mediated by the selectin family. In the second step, ICAM and VCAM bind their chemokine activated integrin ligands resulting in firm adhesion and transendothelial migration. In the last step, when cells are actually attracted to the site of inflammation, for example, skin, the presence of chemokines CCL17 and CCL27, are required 6.

We have generated a mouse model of AD by epidermal expression a Th2 cytokine IL-4 using a basal keratinocyte-specific keratin 14 promoter/enhancer 7. The Tg mice spontaneously developed a pruritic inflammatory skin disease 7 which fulfills the clinical and histological diagnostic criteria for human AD 8. In the lesional skins, we found that there were large numbers of infiltrated inflammatory cells including T cells, mast cells and eosinophils 7, 9, 10. We have furthermore obtained evidences that inflammatory cells may be essential for the development of the inflammation in these IL-4-Tg mice in that as the disease progresses from before onset to early disease and then to late disease phases, the T cells have progressively increased proliferative potential, the percent of activation molecule-bearing T cells progressively increased, and the blockage of CCL27, an important T cell-selective chemokine, leads to partial clearing of the inflammation 11. In the present study, we sought to investigate the roles of adhesion molecules involved in the skin inflammation of the IL-4 Tg mice. Although studies in human AD patients provided indirect evidence in supporting a contributory role of ICAM-1 and VCAM-1 in AD by the findings of enhanced dermal vascular expressions of these two molecules 12, we sought to provide direct evidence for their roles by either physical elimination through gene knockout or by functional blockade through antibody neutralization. Our results demonstrated that VCAM-1, but not ICAM-1, played an important role in the development of skin inflammation in this model.

Results

Significant upregulation of adhesion molecules in the skin of IL-4 Tg mice

In order to elucidate the role of vascular endothelial cell adhesion molecules in the development of skin inflammation in our model, we first sought to screen for the mRNA expressions of various molecules known to be important for skin inflammation. Using reverse transcription followed by quantitative real-time PCR, we found that the mRNAs adhesion molecules in the skin including ICAM-1, VCAM-1, E-selectin, P-selectin, L-selectin, and PSGL-1 mRNAs in the skin of diseased IL-4 Tg mice in the LL stage significantly increased, in comparison to that of non-Tg mice. In addition, the ICAM-1, E-selectin P-selectin, and L-selectin expressions were also significantly increased in the Tg mice of the EL stage (Fig.1A). Western blot analysis further confirmed that protein level of ICAM-1 increased in the skin of EL and LL stages especially in the LL skin, paralleling the increase in mRNA levels (Fig. 1B). We next sought to visualize the upregulation of these molecules at the dermal vascular endothelial cells. Using immunofluorescence microscopy, we determined the presence and the numbers of ICAM-1, VCAM-1, E-selectin, and P-selectin positively stained dermal vessels. While there was no detected expression of these four adhesion molecules in the vessels of non-Tg mice, small numbers of positively stained vessels were detected in the Tg mice at the BO stage (Fig. 2A &B). As the disease progresses from BO stage to EL, and then to LL stage, there was a progressively larger number of positively stained vessels (Fig. 2A&B). Parallel the findings of increase vascular adhesion molecules in the skin, the skin infiltrating leukocytes bearing the L-selectin and PSGL-1 markers were also significantly increased in the diseased skin of Tg mice of the LL stage, compared to that of non-Tg mice (Fig. 2C&D). The results provide indirect evidence that these adhesion molecules may play a role in the inflammation development of our model.

Generation of IL-4-Tg/ICAM-1 knockout mice

Having obtained indirect evidence, we next sought to provide direct evidence pointing to the role of these vascular adhesion molecules in the development of inflammation in our model. Towards that end, we first sought to examine the inflammation development in an ICAM-1−/− mouse line in the context of IL-4 transgene. The scheme for generating the Tg/ICAM-1−/− mice and control littermates were depicted in Fig. 3A. Six groups of mice were generated from this method. The representative genotyping of these mice (with regard to the ICAM-1 gene) is depicted in Fig. 3B.

ICAM-1 knockouts does not lessen the chronic disease severity of IL-4 mice

All the IL-4-Tg mice regardless of ICAM-1 genotype developed skin inflammation and the inflammation was mainly located on the ears. Seven weeks after the onset of the disease, the skin lesions were photographed and severity score recorded. To our surprise, the homozygous Tg/ICAM1−/− and Tg/ICAM +/+ had similar severity scores of skin inflammation (Fig. 4). Similarly there is no difference in disease severity between the heterozygous Tg/ ICAM 1+/− mice and the homozygous IL-4-Tg/ ICAM1+/+ mice (Fig. 4). As expected, none of the Non-Tg mice (non-Tg/ICAM1−/− and non-Tg/ICAM +/+) had developed any skin lesions. The result indicates that ICAM-1 knockout alone does not block

the skin inflammation development in our Tg mice and that there may be a compensatory inflammatory mechanism in the absence of ICAM-1.

Compensatory up-regulation of expressions of ligands of VCAM-1 and P-selectin on T cells

In search for the possible compensatory mechanism that accounts for the undiminished inflammation in the absence of ICAM-1, we sought to examine the surface expression of CD49d [part of the VCAM-1 ligand, VLA-4 (CD49d/CD29)] on CD3+ cell in the skin lesions of the Tg/ICAM-1−/− mice, in comparison to that of the Tg/ICAM-1+/+ mice. As shown in Fig. 5A, 6.5% of CD3+ T cells in the lesional skin of Tg/ICAM-1−/− mice expressed CD49d, much higher than the 2.3% in Tg/ICAM-1+/+ mice ($p<0.01$). T cells expressing similar level of CD24 (P-selectin ligand) in Tg/ICAM-1−/− mice (15.8%) and Tg/ICAM-1+/+ mice (9.4%) ($p>0.05$, Fig. 5A). In the skin-draining lymph nodes of Tg/ICAM-1−/− mice, CD49d expression on CD8+ T cells did have some, but not marked increase compared to Tg/ICAM-1+/+ mice or non-Tg mice, but no increase was observed in CD4+ T cells (Fig. 5B). CD24 expression on these two subsets of T cells in the lymph nodes of Tg/ICAM-1−/− mice, however, was significantly up-regulated compared to Tg/ICAM-1+/+ or non-Tg mice (Fig. 5B). The results suggested that the upregulation of VCAM-1 and P-selectin may play compensatory roles for the skin inflammation in the absence of ICAM-1. Furthermore, the upregulation of CD49d seems to be a local event (in the skin), whereas the upregulation of CD24 may have occurred in the periphery.

Blockade of VCAM-1 delays disease onset and reduces disease severity

Based on the results above showing the upregulation of VCAM-1 ligand in the T cells of the Tg/ICAM-1−/− mice, we hypothesized that blocking the VCAM-1 in IL-4 Tg mice might impede the development of skin inflammation. Towards that end, Tg/ICAM-1−/− and Tg/ICAM-1+/+ mice were treated with monoclonal anti-VCAM-1 neutralization antibody when the mice were 6 weeks old before the disease development and the treatment lasted continuously for 7 weeks. Results demonstrated Tg/ICAM-1+/+ and Tg/ICAM-1 −/− mice started to develop skin lesions at an average of 107 and 96 days of age, respectively, post anti-VCAM-1 administration (Fig. 6B), significantly delayed in comparison to the same groups of mice treated with isotype antibody control (61 and 64 days, $p<0.01$ and <0.05, respectively). There was no significant difference in the time of onset between anti-VCAM-1 treated Tg/ICAM-1+/+ and Tg/ICAM-1−/− mice (Fig. 6B). Interestingly, anti-VCAM-1 treatment significantly reduced the severity of the skin inflammation in Tg/ICAM-1+/+ mice compared to isotype control-treated mice (Fig. 6C). However, anti-VCAM-1 treatment did not reduce disease severity on the Tg/ICAM-1−/− mice (Fig. 6C). Representative clinical phenotypes of these mouse groups were depicted in Fig. 6D.

Histological document of VCAM-1 blockade of inflammatory cells

Having demonstrated that VCAM-1 blockade reduced disease severity and delayed the disease onset in clinical phenotype, we sought to document the histological changes paralleling the reduction in clinical disease severity. By haematoxylin and eosin staining, the skin lesion in anti-VCAM-1-treated mice compared to that of isotype-treated mice, has much less dense dermal inflammatory cell infiltration and thinner epidermis (Fig. 6E). In

particular, the numbers of mast cells (Fig. 6F), eosinophils (Fig. 6E), and CD3+ T cells (Fig. 6G&H), present in the lesion of anti-VCAM-1-treated mice compared to those of isotype-treated mice are substantially reduced ($p<0.01$). In addition, anti-VCAM-1 treatment also significantly down-regulated mRNA expression of an inflammatory cytokine, IL-1β, and an eosinophil chemoattractant, CCL24 (Eotaxin 2) in the lesional skin (Fig. 6H, $p<0.01$). mRNA expression of IL-6 and IL-23 in anti-VCAM-1 treated group were also down-regulated, though not significantly (Fig. 6I). There were no changes of IL-4 between these two groups (data not shown). Furthermore, anti-VCAM-1 treatment significantly reduced the total serum IgE level (180.4ng/ml) compared to that of isotype IgG treated (400.3ng/ml) Tg/ICAM-1++ mice (Fig. 6J, $p<0.01$).

Discussion

In human patients with AD, the endothelial expression of ICAM-1 and VCAM-1 were found to be significantly increased in the healthy-appearing skin (non-lesional skin) of these patients compared to the skin of normal individuals 12. The non-lesional skin showed a further increase of ICAM-1 and VCAM-1 expressions when cultured with medium alone, suggesting that these adhesion molecules are constitutively upregulated in the non-lesional skin of AD possibly because of the cytokines such as IL-4 released by cells in the skin 12. When the skin lesions developed, the endothelial expressions of ICAM-1 and VCAM-1 were found markedly increased in the lesional skin of AD patients compared to normal individuals 13–15. Moreover, some studies suggested that a positive correlation of serum level of soluble ICAM-1 16–20 and VCAM-1 17 with the disease activity of AD. Furthermore, the soluble ICAM-1 level correlated significantly with the total numbers of leukocytes and lymphocytes in AD 16. A positive correlation was also found between the increase in soluble VCAM-1 level and both the clinical activities and the number of monocytes in AD 17. Therefore, it seems that ICAM-1 and VCAM-1 may be critical adhesion molecules in AD. To elucidate the direct role of ICAM-1 in our mouse model of AD, we first crossed this mouse line with ICAM-1−/− mice to generate Tg/ICAM-1−/− mice. However, the results demonstrated that these Tg/ICAM-1−/− mice did not show any signs of reduction of skin inflammation, suggesting that ICAM-1 is not a pivotal adhesion molecule in this model with regard to the control of inflammatory cell migration. Our finding is in fact consistent with the other reports in human AD studies indicating that soluble ICAM-1 level has no correlation with the disease activity 21, 22. Our result also suggests that a functional redundancy exists in the families of adhesion molecules. Based on the previous reports that VCAM-1 is an important factor in human AD 17 and the increase of CD49d, VCAM-1 ligand, on CD3+ T cells in the skin lesions of Tg/ICAM-1−/− mice in the present study (Fig. 5A), we reasoned that VCAM-1 may be the important redundancy of vascular adhesion and that VCAM-1 blockade may help elucidating its true role. Thus, we administered anti-VCAM-1 neutralizing antibody to the Tg/ICAM-1−/− and Tg/ICAM-1+/+ mice before the skin inflammation developed. Result showed that the treatment dramatically delayed the onset of skin inflammation in both Tg/ICAM-1+/+ and Tg/ICAM-1−/− mice, and alleviated the severity of skin lesions in Tg/ICAM-1+/+ mice, but not in Tg/ICAM-1−/− mice. Histologically, skin lesions of anti-VCAM-1 treated Tg/ICAM-1 +/+ mice had significantly less numbers of inflammatory cells infiltrate including T cells, mast cells and

eosinophils. Furthermore, this treatment reduced the mRNA expression of IL-1β, IL-6 and IL-23 in the skin lesions (Fig. 6). IL-1β and IL-6 were two major pro-inflammatory cytokines dramatically increased in the before disease onset skin or lesional skin of Tg mice (9). IL-23 23, a recently discovered IL-12-like T cell cytokine, was also slightly reduced after the treatment, correlating with the reduction of T cell skin infiltration (Fig. 6). In addition, an eosinophil chemoattractant, CCL24 was significantly decreased after anti-VCAM-1 treatment, correlating with the reduction of eosinophil skin infiltration (Fig. 6). Moreover, the anti-VCAM-1 treatment is associated with a reduction of total serum IgE as well as the numbers of mast cell infiltration in skin lesions (Fig. 6). The reason for the decreased serum IgE levl in the anti-VCMA-1-treated mice is not clear. The non-change of skin IL-4 between the anti-VCAM-1-treated and the isotype IgG-treated groups can possibly be explained by the constant presence of baseline IL-4 transgene in both groups. The reduction of these cytokines or chemokine explains the reduced skin inflammation after the treatment. Therefore, in our IL-4 Tg mice, VCAM-1 seems to play a more critical role in controlling the skin inflammation of this animal model. Our data are also in line with the findings of cutaneous delayed hypersensitive studies, showing anti- VCAM-1 or VLA-4 antibody treatment diminished lymphocyte infiltrate in mice and monkeys 24, 25. Further support for a greater importance of VCAM-1 over ICAM-1 included a study in which antibodies against VCAM-1 or VLA-4, but not ICAM-1 and LFA-1, prevented antigen-induced eosinophil infiltration of the mouse trachea, and the same treatments also inhibited CD4+ and CD8+T cell infiltrates more potently than did ICAM-1 or LFA-1 blockade 26. Moreover, antibodies blocking alpha 4-integrin and VCAM-1 both are capable of delaying onset of diabetes and decreased the incidence of the disease in mouse adoptive transfer studies accompanied by markedly reduced lymphocytic infiltration, whereas antibody specific for ICAM-1 had little effect on the onset or incidence of diabetes 27. The reason VCAM-1 plays a greater role in these disease models (delayed hypersensitivity, diabetes, asthma) may be due to the fact that key effector cells in these inflammatory disorders including T cells, monocytes, eosinophils, and basophils that express alpha4-integrin, a ligand for VCAM-1, whereas neutrophils, which are not a key cell type in these disorders, express ICAM-1 ligand but not VCAM-1 ligand 28. The same reason may be applicable to the findings in our model since T cells, eosinophils, and mast cells, but not neutrophils, are the key effector cells in atopic dermatitis 2–4. Although these studies provided encouraging evidence that inhibition of VCAM-1 and VLA-4 pathway mediated adhesion could be a promising strategy in the treatment of autoimmune and allergic inflammatory diseases, these treatments targeting VCAM-1 and VLA-4 did not completely abolish the diseases. Thus, blockade of biologic redundancy involving other important pathways should be also considered, as we also found that there are upregulated expressions of E-selectin, P-selectin, L-selectin, and P-selectin ligand PSGL-1 in the skin lesions. Their direct roles in this animal model remain unclear and are needed to be further investigated.

It is interesting that Tg/ICAM-1−/− mice did not have any reduction in the skin inflammation, when compared to the Tg/ICAM-1+/+ mice. In fact the diseases in Tg/ICAM-1−/− mice are more severe than Tg/ICAM-1+/+ mice, although the difference was not statistically significant (Fig. 4). Moreover, Anti-VCAM-1 treatment reduced the severity of the skin inflammation in Tg/ICAM-1+/+ mice, not in Tg/ICAM-1−/− mice. One possible

explanation is that the substantial increases of VCAM-1 ligand- and P-selectin ligand-bearing T cells as a result of ICAM-1 knockout may have, in a way similar to that of a competitive inhibition, rendered the blockage by a mixed quantity of anti-VCAM-1 less effective in the Tg/ICAM-1−/− mice than that in the Tg/ICAM-1+/+ mice. Alternatively, Knockout of ICAM-1 may have altered the immunological homeostasis in the Tg mice in such a yet-to-be-determined way that resulted in a more severe skin inflammation in Tg/ICAM-1−/− mice. The mechanism needs to be further elucidated.

In summary, we reported in this manuscript the findings that a blockade of VCAM-1 resulted in delay of skin disease onset, reduction of skin disease severity, and reduction of skin infiltration of mast cells, eosinophils, and T cells. Together with our previously reported findings that blockade of T cell-selective chemokine CCL27 reduced the clinical disease phenotype 11 and that the inflammatory disease progression correlated with the increasing inflammatory cell activation and migration towards the skin [10], the data from this Tg mouse AD model support a notion that the inflammation occurred in AD is an inflammatory cell-mediated process.

Materials and Methods

Mice

Four to 12 weeks old IL-4 epidermal transgenic mice (IL-4 Tg) were used in the experiments 7, 9–11, 29. The non-Tg offspring served as age-matched, littermate controls. All mice were housed in the special pathogen-free room and fed with standard water and mouse chew. The study complied with the Animal Care Policies and Procedures of the University of Illinois at Chicago.

IL-4-Tg/ICAM-1 knockout (Tg/ICAM-1−/−) mice were generated by crossing our IL-4-Tg mice (in CByB6 strain) with a commercially available homozygous ICAM-1−/− mouse line (Stock No. 002867, Jackson Lab, Bar Harbor, ME, USA). The homozygous ICAM-1−/−mice were first mated with IL-4-Tg mice to produce heterozygous Tg /ICAM-1+/− and non-Tg/ICAM-1+/− mice. The subsequent cross between heterozygous Tg /ICAM-1+/− and non-Tg/ICAM-1+/− mice produced six (6) groups of mice: 1). homozygous Tg/ICAM-1−/− mice; 2). homozygous Tg/ICAM-1+/+ mice; 3). heterozygous Tg/ICAM-1+/− mice; 4). homozygous non-Tg/ICAM-1−/− mice; 5). homozygous non-Tg/ICAM-1+/+ mice; and 6). heterozygous non-Tg/ICAM-1+/− mice. The first five groups of mice were included in our experimental protocol. The development of skin lesions in all five mice groups were closely observed three times per week. All mice were sacrificed 7 weeks after onset of the skin inflammation. The severity score for each mouse was recorded as described previously 29.

Genotyping

For ICAM-1 genotyping, genomic DNA extracted from tail clipping was genotyped by PCR for homozygous knockout (ICAM-1−/−), heterozygous (ICAM-1+/−), or wild type (ICAM-1+/+) using a primer pair that detects neo gene in the ICAM-1 target mutation procedure: 5’-CTGAATGAACTGCAGGACGA-3’; 5’-ATACTTTCTCGGCAGGAGCA-3’ and a primer pair that detects the wild type gene: 5 ’-

CAGCTACCATCCCAAAGCTC-3’ ; 5 ’-GTAGACTGTTAAGGTCCTCTG-3’. The primer sequences and PCR conditions were obtained from Jackson Lab with the following parameters: Preheating at 94 °C for 1.5 min., followed by a 35-cycles of 94 °C 30 sec., 60 °C 30 sec., 72 °C 30 sec., then by an extension of 72 °C 2 min. The products were run on 1.8% agrose gel and then examinations and photos were conducted under UV light transillumination. The method for IL-4 genotyping was published previously 9. As we have previously determined that IL-4 transgene copy numbers do not correlate with disease severity 29, heterozygous IL-4-transgenic mice were used in our experiment.

Disease phenotype classification

Skin lesions from IL-4 Tg mice that have been developed for one week or shorter in duration were defined as early lesion (EL). Skin lesions that have been developed for three weeks or longer in duration were defined as late lesion (LL). Tg mice before any skin lesion surfaces were defined as before disease onset (BO) as described in our previous publications 9–11, 29.

Production of monoclonal antibody against mouse VCAM-1

Hybridoma producing anti-mouse VCAM-1 neutralizing monoclonal antibody (clone m/k-2.7, rat IgG1) was purchased from ATCC (Manassas, VA, USA). Cells were cultured in RPMI 1640 with 10% FCS and 0.05mM 2-mercaptoethanol. To produce an isotype control antibody, hybridoma AIIB2 (rat IgG1, anti-human integrin β-1 antibody, without cross reaction with mouse tissue) was purchased from the Developmental Studies Hybridoma Bank, University of Iowa, Iowa City, IA, USA). Cells were cultured in Iscove’s Dulbecco's modified Eagle's medium as instructed. The proteins in culture supernatant were precipitated by ammonium sulfate, and then the IgG antibodies were purified using protein G Sepharose 4 column (Amersham Biosciences, Piscataway, NJ, USA). The purity of the IgGs was determined by SDS-PAGE to be > 98 % (Data not shown).

Anti VCAM-1 treatment and Score of the disease severity

Tg/ICAM-1+/+ and Tg/ICAM-1−/− mice were treated with anti-VCAM-1 neutralizing antibody (0.5mg/mouse, intra-peritoneal administration, every 5 days, n=10 for each group) started from 6 weeks of age before the skin lesions developed. This administration route and dose was chosen according to a protocol that successful blockaded the VCAM-1 function 30. The treatment was terminated 7 weeks after the disease onset (Fig. 6A). For isotype control, two other groups of these mice (n=10 for each group) received the same amount of non-specific rat IgG1 treatment for the same treatment duration. The time of disease onset and severity scores were recorded as described 29.

Briefly, it was determined by the number of location of skin affected by inflammatory skin lesions. The presence of inflammation, scale, or skin lesions in each of the following area, will be assigned one numerical number: left ear, right ear, face, eye, trunk, left leg, right leg, tail. The severity score of the disease will be the sum of total numerical numbers of a given mouse 29.

Quantitative Real-Time Polymerase Chain Reaction (PCR)

Total RNAs from skin tissues of Non-Tg, Tg-BO, Tg-EL, and Tg-LL mice were extracted using Trizol (Invitrogen, Carlsbad, CA, USA) and reverse transcribed to cDNA using Retro-script RT kit (Ambion, Austin, TX, USA) as previously described 9. For real-time PCR, we used SYBR green PCR reaction mix (Bio-Rad, Hercules, CA, USA) with ICAM-1, VCAM-1, E-Selectin, P-selectin, L-selectin, and PSGL-1 gene-specific primers (listed below) by method described previously 9. cDNA templates of individual samples or ten-fold serial dilutions of the plasmid standards with concentrations ranging from 5×10 to 5×10^6 copies. For all adhesion molecules, identical thermal cycling conditions were used: 15s at 95°C and 1 min at 60°C with total of 40 cycles followed by a melting curve data collection set up to identify the non-specific products or primer-dimers. The copy number of the gene present in the mRNA extract of the tissue was automatically determined by a software program in Mx3000p real-time PCR unit (Stratagene, La Jolla, CA) according to the standard curve of the plasmid DNA. In order to normalize for cDNA synthesis efficiencies and RNA input amounts, the highest copy number of GAPDH of all samples was divided by copy numbers of GAPDH in an individual sample to give a calculating factor. The normalized adhesion molecule gene copy number was determined by multiplying this calculating factor with the gene copy number obtained from standard curve generated by PCR. Primers used include: E-Selectin: Forward: 5'-TTT-CAA-TGC-AAT-GAG-GGC-TTT-3', Reverse: 5'-GGA-CGT-CAA-GGC-TTG-GAC-AT-3'; P-Selectin: Forward: 5'-GCC-AGT-TCA-TGT-GCG-ATG-AA-3', Reverse: 5'-GGC-GAA-GAT-TCC-TGG-ACA-CTT-3'; VCAM-1: Forward: 5'-GTG-AAG-ATG-GTC-GCG-GTC-TT-3', Reverse: 5'-GGCCATGGAGTCACCGATT-3'; ICAM-1: Forward: 5'-CCG-CAG-GTC-CAA-TTC-ACA-CT-3', Reverse: 5'-TCC-AGC-CGA-GGA-CCATAC-AG-3'; PSLG-1, Forward: 5'-ATC-TCA-TCC-CGG-TGA-AGC-AA-3', Reverse: 5'-TTC-CGC-ACT-GGG-TAC-ATG-TG-3'; L-Selectin, Forward: 5'-GAC-GCC-TGT-CAC-AAA-CGA-AA-3', Reverse: 5'-GCC-CGT-AAT-ACC-CTG-CAT-CA-3'. Primers used for GAPDH were published previously 31. In addition, relative quantities of cytokine mRNAs (IL-1 β, IL-4, IL-6, IL-23) and chemokine mRNAs (CCL24/Eotaxin 2) in the skin lesions between Tg/ICAM-1++/anti-VCAM-1 and Tg/ICAM-1++/IgG groups were also determined by semi-quantitative real-time PCR as described in 9. Primers used for IL-1β, IL-4, IL-6, were published previously 9. Primers for CCL24 and IL-23 were previously published in references 32 and 33, respectively.

Western Blot Analysis

Mouse ears were collected from Non-Tg, Tg-BO, Tg-EL, and Tg-LL mice and tissues were then homogenized in the presence of a multiple protease inhibitors (Sigma, St. Louis, MO)-containing lysing solution. After centrifugation, supernatants were collected and the amount of proteins was quantified by a protein assay (Bio-rad). The identical amount of proteins (140μg) from each sample group was loaded in a 4–20% Tris-glycine acrylamide gel (Bio-rad). The separated proteins were transferred to nitrocellulose membrane. Membrane was first blocked with an infrared scanner-specific blocking buffer (Li-Cor, Lincoln, Nebraska, USA), then a rat anti-mouse ICAM-1 (Clone YN1/1.7.4, 0.25μg/ml, Southern Biotech, Birmingham, Alabama, USA) was applied to the membrane at room temperature followed

by incubation of an Alexa Fluor 680-labeled goat anti-rat IgG (Invitrogen). Image was acquired using Odyssey infrared scanner (Li-Cor).

Histology

Seven weeks after anti-VCAM-1 or isotype treatment in Tg/ICAM-1+/+ mice, lesional skin samples were collected, fixed in formalin, and processed for haematoxylin/eosin and Giemsa staining as described in reference 9. Mast cells in Giemsa stained sections and eosinophils in haematoxylin and eosin stained sections were counted per high power field (HPF, x40 objective lens for mast cells and x50 objective lens for eosinophils). Five fields of each section were counted independently by two investigators (L.Chen and L. S. Chan). The average numbers counted by these two investigators were used as final count (n=5).

Immunofluorescence Microscopy

All tissue samples were taken from ears of Non-Tg, Tg-BO, Tg-EL and Tg-LL mice. The tissue samples were treated with 0.2% paraformaldehyde overnight, followed by 30% sucrose in PBS. The tissues were embedded in Tissue-Tek OCT compound (Sakura Finetechnical, Tokyo, Japan) and snap frozen with liquid nitrogen. 8 μm sections were cut using a Leica CM 1850 cryostat (Leica Microsystems, Nussloch, Germany). The primary antibodies including hamster anti-mouse ICAM-1 (Clone 3E2, 1/500 dilution), rat anti-mouse VCAM-1 (Clone 429, 1/700 dilution), rat anti-mouse E-selectin (Clone 10E9.6, 1/200 dilution), rabbit anti-human P-selectin (Clone RB40.34, 1/200 dilution, cross-react with mouse P-selectin), rat anti-mouse L-selectin (Clone MEL-14, 1/500 dilution), and rat anti-mouse PSGL-1 (Clone 2PH1, 1/2000 dilution) (BD Biosciences, San Diego, CA, USA), were then applied to the sections. After wash, the sections were incubated with Alexa fluor 488 conjugated secondary antibodies including goat anti-rat IgG, goat anti-hamster IgG, goat anti-rabbit IgG (Invitrogen). After staining, the sections on each slide were mounted using glycerol/PBS at a 1:1 (v:v) ratio, and examined under an Olympus BX60 fluorescence microscope with a high power objective lens (40x). Five different areas for each tissue sample were counted to determine the number of stained vessels. The average number of positively stained vessels was then calculated as vessels per high powered field (HPF). Fifteen samples from each group (Non-Tg, Tg-BO, Tg-EL, and Tg-LL) were included in this study.

Immunohistochemistry

Immunohistochemistry staining of formalin-fixed paraffinized skin samples were performed as previously described with minor modifications 34. The primary antibody used was a monoclonal rat anti-mouse CD3 (Southern Biotech, Birmingham, AL). Five different areas of each sample were counted per HPF and averaged (n=5).

FACS analyses

For analysis of CD24 and CD49d on CD3 cells in the skin lesions, single cell suspensions and immuno-staining for the Tg/ICAM-1−/− and Tg/ICAM-1+/+ lesional skin 7 weeks after the onset of the skin inflammation were prepared as described previously by Elbe-Burger et al35. We also used the same method to analyze intercellular cytokine expression in CD3+

and MHC II cells from skin lesions9. Cells were first incubated with Fc blocker (anti-CD16/32) (eBioscience, San Diego, CA, USA), then with FITC anti-CD3 (Clone 145-2C11), and PE anti-CD24 (Clone 30-F1) or CD49d (Clone R1-2) (eBioscience), and finally analyzed by Calibur FACS system (BD Bioscience). For analyses of CD24 and CD49d on CD4 and CD8 T cells in the skin draining lymph nodes of Tg/ICAM-1−/− , Tg/ICAM-1+/+, non-Tg/ICAM-1−/− and non-Tg/ICAM-1+/+ mice, single cells suspensions were stained with FITC anti-CD4 (Clone RM4-5)/CD8 (Clone 53-6.7) (eBioscience) and PE anti-CD24 or CD49d, then analyzed by FACS. In all experiments, samples with FITC or PE-conjugated isotype controls were also analyzed. All Antibodies were used at a final concentration of 5μg/ml. The reason for examining CD24 and CD49d on CD3+ cells instead of on CD4+ and CD8+ subsets in the skin lesions was that it was difficult to obtain enough CD4+ and CD8+ cells from the skin to analyze.

ELISA

Total serum IgE in anti-VCAM-1 treated Tg/ICAM-1++ mice and IgG control mice (n=10 in each group) was determined using a commercially available mouse IgE ELISA kit (Bethyl Laboratoris, INC, Montgomery, TX, USA).

Statistical analyses

All experimental data were expressed as mean ± SD. The significance of the variation among different groups was determined by One-Way ANOVA Analysis and the difference between two groups was determined by Tukey-Kramer Multiple Comparison Test using GraphPad Instat Software (San Diego, CA, USA). *p* value <0.05 was considered to be significantly different.

Acknowledgements

We thank Mr. Prakash Venkataramani and Dr. Valeria I. Barriuso for their technical help and helpful discussion. This work is supported in part by NIH grants (R01 AR47667, R03 AR47634, and R21 AR48438, L. S. Chan) and Albert H. and Mary Jane Slepyn Fellowship Fund (L. Chen).

Abbreviations

AD	atopic dermatitis
Tg	IL-4-transgenic
Non-Tg	non-transgenic
Tg-BO	transgenic mouse at before skin disease onset
Tg-EL	transgenic mouse with early skin lesion (lesion onset for one week or shorter)
Tg-LL	transgenic mouse with late skin lesion (lesion onset for three weeks or longer)
ICAM-1+/+	ICAM-1 wild type
ICAM-1−/−	homogyzous ICAM-1 knockout

ICAM-1+/− heterogyzous ICAM-1 knockout

References

1. Leung DY, Boguniewicz M, Howell MD, Nomura I, Hamid QA. New insights into atopic dermatitis. J Clin Invest. 2004; 113(5):651–657. [PubMed: 14991059]
2. Leung DY, Bieber T. Atopic dermatitis. Lancet. 2003; 361(9352):151–160. [PubMed: 12531593]
3. Cooper KD. Atopic dermatitis: recent trends in pathogenesis and therapy. J Invest Dermatol. 1994; 102(1):128–137. [PubMed: 8288906]
4. Reinhold U, Kukel S, Goeden B, Neumann U, Kreysel HW. Functional characterization of skin-infiltrating lymphocytes in atopic dermatitis. Clin Exp Immunol. 1991; 86(3):444–448. [PubMed: 1721013]
5. Steinhoff M, Steinhoff A, Homey B, Luger TA, Schneider SW. Role of vasculature in atopic dermatitis. J Allergy Clin Immunol. 2006; 118(1):190–197. [PubMed: 16815154]
6. Schon MP, Zollner TM, Boehncke WH. The molecular basis of lymphocyte recruitment to the skin: clues for pathogenesis and selective therapies of inflammatory disorders. J Invest Dermatol. 2003; 121(5):951–962. [PubMed: 14708592]
7. Chan LS, Robinson N, Xu L. Expression of interleukin-4 in the epidermis of transgenic mice results in a pruritic inflammatory skin disease: an experimental animal model to study atopic dermatitis. J Invest Dermatol. 2001; 117(4):977–983. [PubMed: 11676841]
8. Hanifin JM, Rajka G. Diagnostic features of atopic dermatitis. Acta Derm Venereol. 1980; 92:44–47.
9. Chen L, Martinez O, Overbergh L, Mathieu C, Prabhakar BS, Chan LS. Early up-regulation of Th2 cytokines and late surge of Th1 cytokines in an atopic dermatitis model. Clin Exp Immunol. 2004; 138(3):375–387. [PubMed: 15544612]
10. Chen L, Martinez O, Venkataramani P, Lin SX, Prabhakar BS, Chan LS. Correlation of disease evolution with progressive inflammatory cell activation and migration in the IL-4 transgenic mouse model of atopic dermatitis. Clin Exp Immunol. 2005; 139(2):189–201. [PubMed: 15654817]
11. Chen L, Lin SX, Agha-Majzoub R, Overbergh L, Mathieu C, Chan LS. CCL27 is a critical factor for the development of atopic dermatitis in the keratin-14 IL-4 transgenic mouse model. Int Immunol. 2006; 18(8):1233–1242. [PubMed: 16735375]
12. Jung K, Linse F, Heller R, Moths C, Goebel R, Neumann C. Adhesion molecules in atopic dermatitis: VCAM-1 and ICAM-1 expression is increased in healthy-appearing skin. Allergy. 1996; 51(7):452–460. [PubMed: 8863922]
13. Boone M, Lespagnard L, Renard N, Song M, Rihoux JP. Adhesion molecule profiles in atopic dermatitis vs. allergic contact dermatitis: pharmacological modulation by cetirizine. J Eur Acad Dermatol Venereol. 2000; 14(4):263–266. [PubMed: 11204513]
14. Lugovic L, Cupic H, Lipozencic J, Jakic-Razumovic J. The role of adhesion molecules in atopic dermatitis. Acta Dermatovenerol Croat. 2006; 14(1):2–7. [PubMed: 16603095]
15. Sigurdsson V, de Vries IJ, Toonstra J, Bihari IC, Thepen T, Bruijnzeel-Koomen CA, et al. Expression of VCAM-1, ICAM-1, E-selectin, and P-selectin on endothelium in situ in patients with erythroderma, mycosis fungoides and atopic dermatitis. J Cutan Pathol. 2000; 27(9):436–440. [PubMed: 11028813]
16. Koide M, Tokura Y, Furukawa F, Takigawa M. Soluble intercellular adhesion molecule-1 (sICAM-1) in atopic dermatitis. J Dermatol Sci. 1994; 8(2):151–156. [PubMed: 7841158]
17. Koide M, Furukawa F, Tokura Y, Shirahama S, Takigawa M. Evaluation of soluble cell adhesion molecules in atopic dermatitis. J Dermatol. 1997; 24(2):88–93. [PubMed: 9065702]
18. Hirai S, Kageshita T, Kimura T, Tsujisaki M, Okajima K, Imai K, et al. Soluble intercellular adhesion molecule-1 and soluble E-selectin levels in patients with atopic dermatitis. Br J Dermatol. 1996; 134(1):657–661. [PubMed: 8733366]

19. Kojima T, Ono A, Aoki T, Kameda-Hayashi N, Kobayashi Y. Circulating ICAM-1 levels in children with atopic dermatitis. Ann Allergy. 1994; 73(4):351–355. [PubMed: 7944004]
20. Wuthrich B, Joller-Jemelka H, Kagi MK. Levels of soluble ICAM-1 in atopic dermatitis. A new marker for monitoring the clinical activity? Allergy. 1995; 50(1):88–89. [PubMed: 7741194]
21. Yamashita N, Kaneko S, Kouro O, Furue M, Yamamoto S, Sakane T. Soluble E-selectin as a marker of disease activity in atopic dermatitis. J Allergy Clin Immunol. 1997; 99(3):410–416. [PubMed: 9058698]
22. Wolkerstorfer A, Laan MP, Savelkoul HF, Neijens HJ, Mulder PG, Oudesluys-Murphy AM, et al. Soluble E-selectin, other markers of inflammation and disease severity in children with atopic dermatitis. Br J Dermatol. 1998; 138(3):431–435. [PubMed: 9580795]
23. Hao JS, Shan BE. Immune enhancement and anti-tumour activity of IL-23. Cancer Immunol Immunother. 2006; 55(11):1426–1431. [PubMed: 16676182]
24. Silber A, Newman W, Sasseville VG, Pauley D, Beall D, Walsh DG, et al. Recruitment of lymphocytes during cutaneous delayed hypersensitivity in nonhuman primates is dependent on E-selectin and vascular cell adhesion molecule 1. J Clin Invest. 1994; 93(4):1554–1563. [PubMed: 7512984]
25. Chisholm PL, Williams CA, Lobb RR. Monoclonal antibodies to the integrin alpha-4 subunit inhibit the murine contact hypersensitivity response. Eur J Immunol. 1993; 23(3):682–688. [PubMed: 8449216]
26. Nakajima H, Sano H, Nishimura T, Yoshida S, Iwamoto I. Role of vascular cell adhesion molecule 1/very late activation antigen 4 and intercellular adhesion molecule 1/lymphocyte function-associated antigen 1 interactions in antigen-induced eosinophil and T cell recruitment into the tissue. J Exp Med. 1994; 179(4):1145–1154. [PubMed: 7511681]
27. Baron JL, Reich EP, Visintin I, Janeway CA Jr. The pathogenesis of adoptive murine autoimmune diabetes requires an interaction between alpha 4-integrins and vascular cell adhesion molecule-1. J Clin Invest. 1994; 93(4):1700–1708. [PubMed: 7512990]
28. Hemler ME. VLA proteins in the integrin family: structures, functions, and their role on leukocytes. Annu Rev Immunol. 1990; 8:365–400. [PubMed: 2188667]
29. Chen L, Lin SX, Overbergh L, Mathieu C, Chan LS. The disease progression in the keratin 14 IL-4-transgenic mouse model of atopic dermatitis parallels the upregulations of B cell activation molecules, proliferation, and surface and serum IgE. Clin Exp Immunol. 2005; 142:21–30. [PubMed: 16178852]
30. Kootstra CJ, Van Der Giezen DM, Van Krieken JH, De Heer E, Bruijn JA. Effective treatment of experimental lupus nephritis by combined administration of anti-CD11a and anti-CD54 antibodies. Clin Exp Immunol. 1997; 108(2):324–332. [PubMed: 9158106]
31. Giulietti A, Overbergh L, Valckx D, Decallonne B, Bouillon R, Mathieu C. An overview of real-time quantitative PCR: applications to quantify cytokine gene expression. Methods. 2001; 25(4): 386–401. [PubMed: 11846608]
32. Maatta J, Majuri ML, Luukkonen R, Lauerma A, Husgafvel-Pursiainen K, Alenius H, et al. Characterization of oak and birch dust-induced expression of cytokines and chemokines in mouse macrophage RAW 264.7 cells. Toxicology. 2005; 215(1–2):25–36. [PubMed: 16122864]
33. Broberg EK, Setala N, Eralinna JP, Salmi AA, Roytta M, Hukkanen V. Herpes simplex virus type 1 infection induces upregulation of interleukin-23 (p19) mRNA expression in trigeminal ganglia of BALB/c mice. J Interferon Cytokine Res. 2002; 22(6):641–651. [PubMed: 12162874]
34. Jean-Baptiste S, O'Toole EA, Chen M, Guitart J, Paller A, Chan LS. Expression of eotaxin, an eosinophil-selective chemokine, parallels eosinophil accumulation in the vesiculobullous stage of incontinentia pigmenti. Clin Exp Immunol. 2002; 127(3):470–478. [PubMed: 11966763]
35. Elbe-Burger A, Egyed A, Olt S, Klubal R, Mann U, Rappersberger K, et al. Overexpression of IL-4 alters the homeostasis in the skin. J Invest Dermatol. 2002; 118(5):767–778. [PubMed: 11982753]

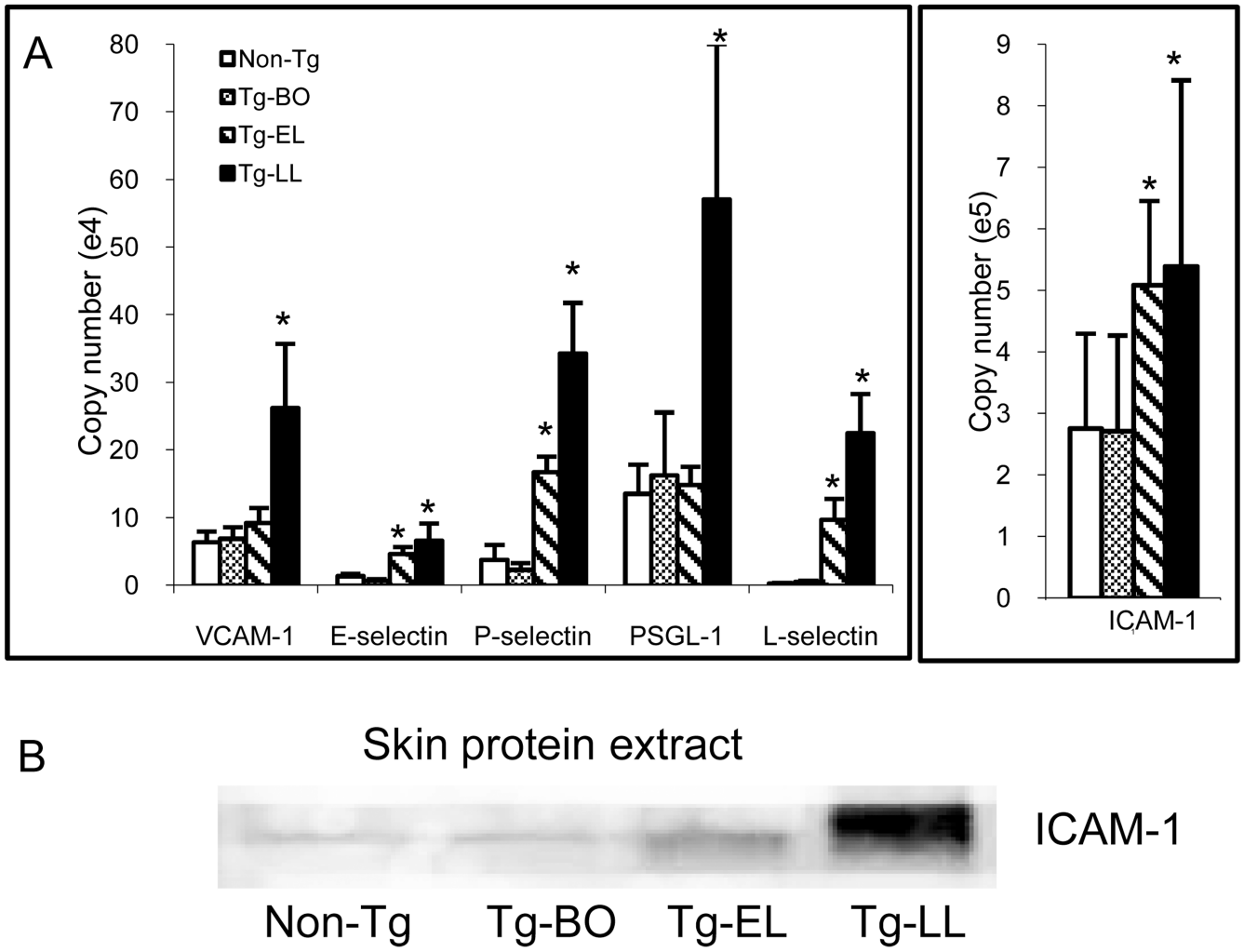

Figure 1.

Upregulations of adhesion molecules in the skin of IL-4-Tg mice parallel the disease progression. (A) mRNA expressions: Total RNA from skin samples of Non-Tg, Tg-BO, Tg-EL, and Tg-LL mice were extracted and reverse transcripted to cDNA. Relative quantities of ICAM-1, VCAM-1, E-selectin, P-selectin, PSGL-1, and L-selectin mRNA expression were determined by quantitative real time PCR. (B) Protein expressions: Skin protein extracts were obtained from the skins of Non-Tg, Tg-BO, Tg-EL, and Tg-LL mice. After the SES-PAGE and nitrocellulose membrane protein transfer, ICAM-1 was detected by an anti ICAM-1 antibody followed by an Alexa Fluor 680-labeled secondary antibody. The membrane was then scanned by an Odyssey infrared scanner (Li-cor). *$p<0.05$ compared to non-Tg mice.

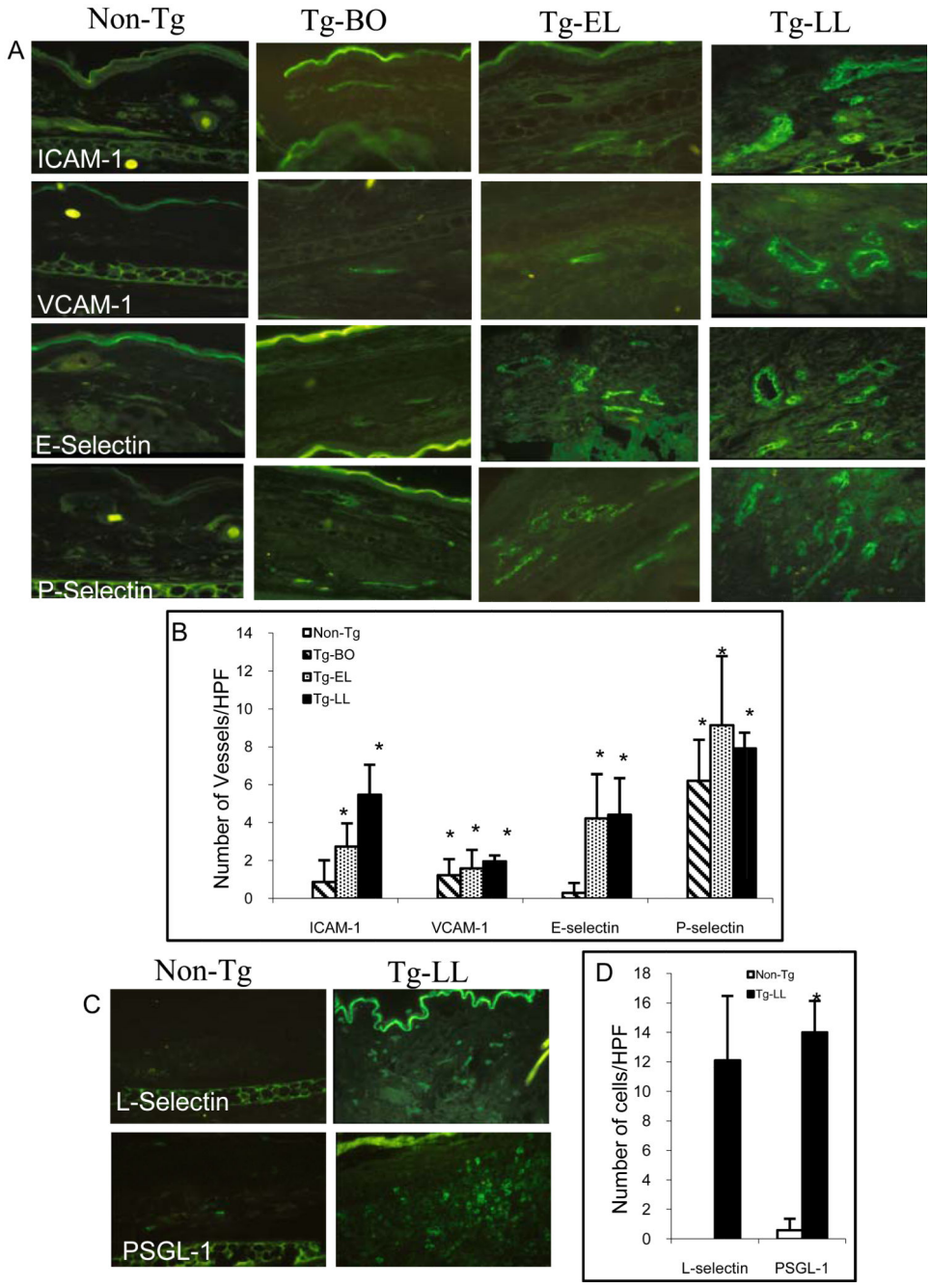

Figure 2.

The increase of number of adhesion molecules-positive dermal blood vessels and inflammatory cells correlate with the disease progress. (A) Representatives of immunofluorescence photomicrographs of positively stained ICAM-1, VCAM-1, E-selectin, and P-selectin in the skin sections of Non-Tg, Tg-BO, Tg-EL and Tg-LL mice (Original magnification X100). (B) Bar graph presentations of the average number of positively stained vessels (per HPF). (C) Representatives of immunofluorescence photomicrographs of positively stained L-selectin and PSGL-1 in the skin sections of Non-Tg and Tg-LL mice

(Original magnification X100). (D) Bar graph presentations of the average number of positively stained inflammatory cells for L-selectin and PSGL-1. * $p<0.001$ compared to non-Tg mice.

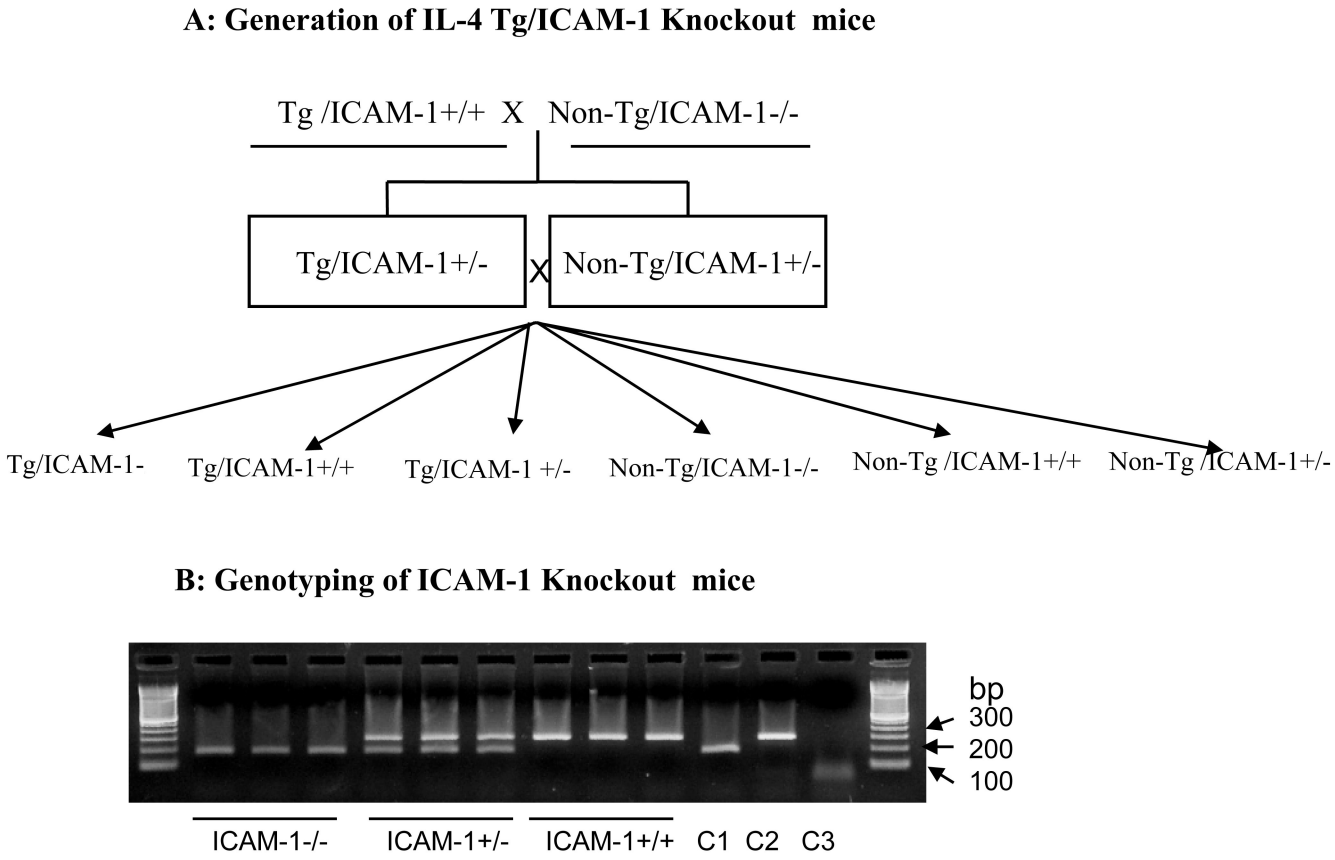

Figure 3.

Generation and genotyping of Tg/ICAM-1 knockout mice. (A) Scheme for the generation of Tg/ICAM-1 knockout mice: IL-4-Tg mice were crossed with purchased homozygous ICAM-1−/− mice to produce heterozygous Tg/ICAM-1+/− and non-Tg/ICAM-1+/− mice. The subsequent cross between heterozygous Tg/ICAM-1+/− mice and heterozygous non-Tg/ICAM-1+/− mice produced homozygous Tg/ICAM-1−/− mice (our testing group), non-Tg/ICAM-1−/− mice (our negative control) and the other littermate control mouse groups (B) Genotyping of Tg/ICAM-1 KO mice: Genotyping of ICAM-1 mice (homozygous and heterozygous) was performed according to the instructions from the ICAM-1−/− mice vendor. Photo shows the results of ICAM-1 genotyping, ICAM-−/−, ICMA-1+/−, and ICAM-1+/+ (3 mice for each group) resulted from our crossing. C1: PCR product using control DNA for ICAM-1−/−, C2: PCR product using control for ICAM-1+/+ (wild type), C3: PCR product without DNA template (negative control).

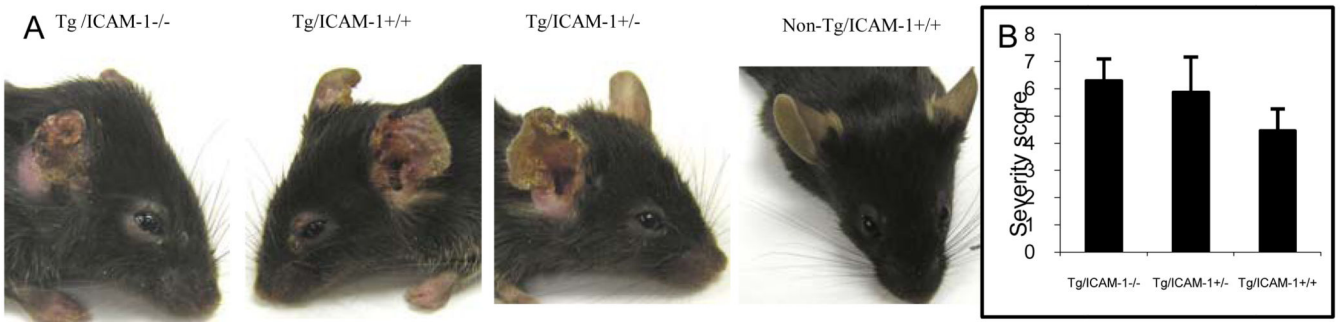

Figure 4.

Clinical phenotypes of IL-4-Tg mice with normal or deficient ICAM-1. (A) Representative clinical phenotypes of Tg/ICAM-1−/−, Tg/ICAM-1+/+, Tg/ICAM-1+/− (7 weeks after disease onset), and non-Tg/ICAM-1+/+ mice. (B) Comparison of skin inflammation severity scores of Tg/ICAM-1−/−, Tg/ICAM-1+/−, and Tg/ICAM-1+/+ mouse groups (7 weeks after disease onset. N=15 for each group), $p>0.05$ (among these three groups).

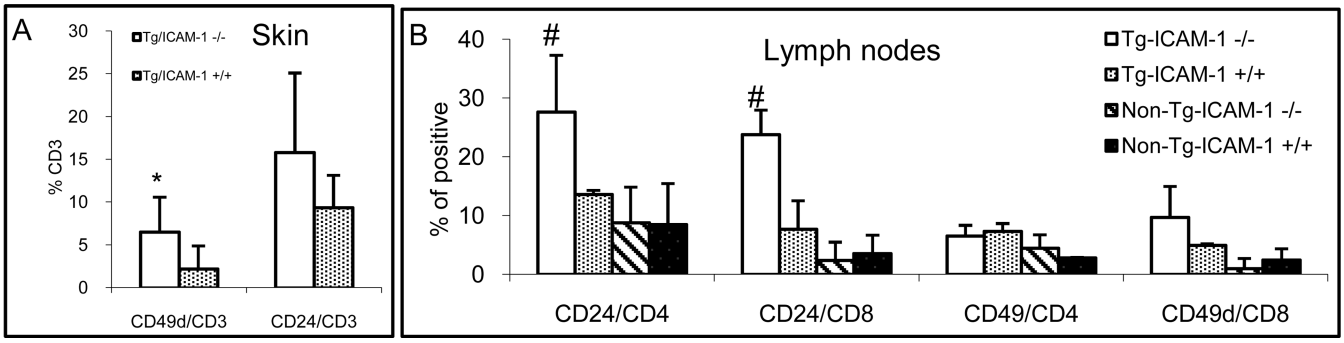

Figure 5.

Upregulation of CD49d and CD24 on T cells in the lesional skin and skin-draining lymph nodes. Single cell suspensions from lesional skin (A) and skin draining lymph nodes (B) of Tg/ICAM-1−/− and Tg/ICAM-1+/+ mice were stained with FITC-CD3/PE-CD24/PE-CD49d for skin cells (A), and FITC-CD4/FITC-CD8/PE-CD49d/PE-CD24 for lymph node (B), then analyzed by flow cytometry. Results were the averages of three experiments. *$p<0.01$ compared to Tg/ICAM-1+/+ mice in A; # $p<0.05$ compared to Tg/ICAM-1+/+, or non-Tg/ICAM-1+/+, or non-Tg/ICAM-−/− mice in B.

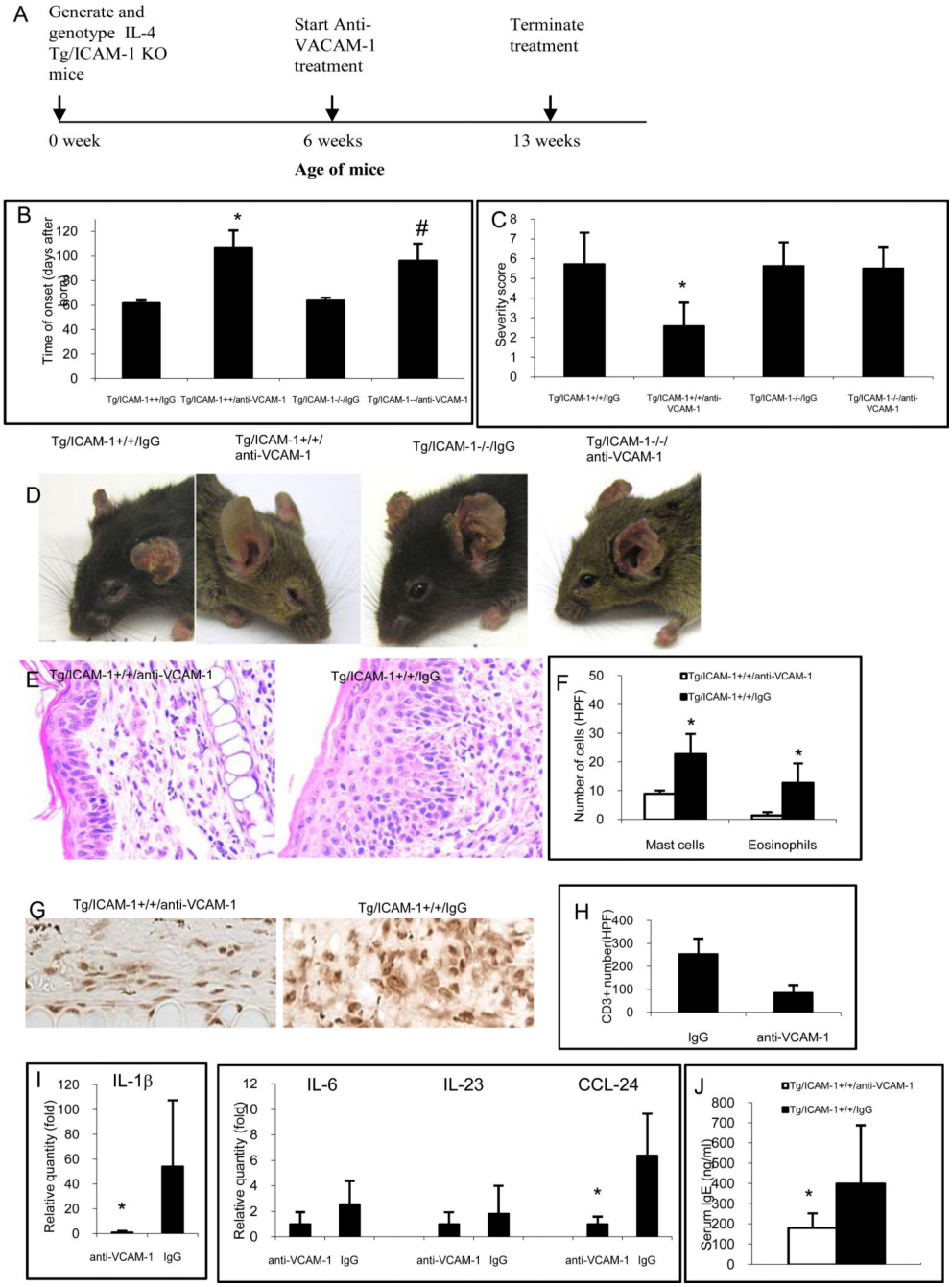

Figure 6.

VCAM-1 neutralizing antibody reduces skin inflammation in Tg ICAM-1+/+ not in Tg ICAM-1−/− mice. (A) Timeline of anti-VCAM-1 treatment. (B) Neutralizing antibody to VCAM-1 delays the onset of skin inflammation and reduces the severity of skin disease (C) in comparison to those mice treated by non-specific isotype control (* $p<0.01$, #$p<0.05$ compared to their isotype control antibody treated groups. (D) Representative clinical phenotypes of Tg/ICAM-1−/− and Tg/ICAM-1+/+ mice treated either with anti-VCAM-1 or isotype control. (E) Histopathology of Tg/ICAM-1+/+ mice treated either with anti-

VCAM-1 or isotype control (Hematoxylin/eosin stain, Original magnification X100). (F) Mast cells and eosinophils in the dermis after anti-VCAM-1 or isotype control treatment in Tg/ICAM-1+/+ mice. N=5 for each group, *p<0.01 compared to IgG control groups). (G&H) CD3+ T cell infiltrates in Tg/ICAM-1+/+ mice treated either with anti-VCAM-1 or isotype control. * p<0.01 compared to IgG control groups (G, Original magnification X250). (I) mRNA expression of IL-1β, IL-6, IL-23 and CCL24 in the lesional skin of anti-VCAM-1 treated Tg/ICAM-1++ mice. * p<0.01 compared to IgG control groups. (J) Total serum IgE in anti-VCAM-1 treated Tg/ICAM-1++ mice. n=10 in each group, *p<0.05 compared to IgG control groups.